

# Enhanced Droplet Analysis Using Generative Adversarial Networks

Tan-Hanh Pham

Department of Mechanical and  
Civil Engineering, Florida Institute of  
Technology, USA  
Email: tpham2023@my.fit.edu

Kim-Doang Nguyen\*

Department of Mechanical and  
Civil Engineering, Florida Institute of  
Technology, USA  
Email: knguyen@fit.edu

**Abstract**—Precision devices play an important role in enhancing production quality and productivity in agricultural systems. Therefore, the optimization of these devices is essential in precision agriculture. Recently, with the advancements of deep learning, there have been several studies aiming to harness its capabilities for improving spray system performance. However, the effectiveness of these methods heavily depends on the size of the training dataset, which is expensive and time-consuming to collect. To address the challenge of insufficient training samples, this paper proposes an alternative solution by generating artificial images of droplets using generative adversarial networks (GAN). The GAN model is trained by using a small dataset captured by a high-speed camera and capable of generating images with progressively increasing resolution. The results demonstrate that the model can generate high-quality images with the size of  $1024 \times 1024$ . Furthermore, this research leverages recent advancements in computer vision and deep learning to develop a light droplet detector using the synthetic dataset. As a result, the detection model achieves a 16.06% increase in mean average precision (mAP) when utilizing the synthetic dataset. To the best of our knowledge, this work stands as the first to employ a generative model for augmenting droplet detection. Its significance lies not only in optimizing nozzle design for constructing efficient spray systems but also in addressing the common challenge of insufficient data in various precision agriculture tasks. This work offers a critical contribution to conserving resources while striving for optimal and sustainable agricultural practices.

**Keywords:** Polyps, Colonoscopy, Medical image analysis, Deep learning, Vision transformers.

## I. INTRODUCTION

### A. Motivation

In the current era of global environmental transformations caused by climate change, it is imperative to prioritize global sustainability and food security to ensure the well-being and support the livelihoods of humanity. In agriculture, numerous innovations leverage modern technologies to enhance productivity while minimizing environmental impact. Beyond the natural conditions of the environment, technology emerges as a pivotal player in agriculture, empowering the system to conserve resources and operate with greater efficiency. One noteworthy innovation is the use of spray systems in nurturing plants, considered a highly effective priority tool. These systems, when integrated with other technologies, not only save farmers time but also enhance synchronization on their farms. As depicted in Figure 1, a spray system can

uniformly distribute substances into plants, facilitating optimal nutrient absorption or distributing pesticides to help crops minimize diseases.

Precision spraying systems play a crucial role in modern agriculture due to their impact on droplet drift and efficacy. Therefore, to enhance precision in spraying systems, it's vital to optimize spray nozzles. This involves adjusting nozzle parameters to change the characteristics of released droplets and make them suitable to each crop's unique needs and environmental conditions. There are several methods to measure the droplet characteristics. Traditional optical measurement methods include high-speed photography and laser imaging [1, 2]. For example, one common method estimates droplet size by spraying colored water on a white sheet and then analyzing the resultant patterns [3, 4]. These methods are often highly manual, require delicate setups, and are associated with high operating costs.

Recently, with the advent of advanced machine learning, [5] developed a novel tool to estimate the size and velocity of droplets sprayed from agricultural nozzles. Moreover, [6] developed a lightweight droplet detector that can be easily incorporated into sensing systems. Despite these advancements, these models are heavily dependent on the size of the datasets used for model training. However, gathering data to train machine learning models in most precision agriculture applications remains a time-consuming, labor-intensive, and expensive process.

Motivated by these challenges, this paper utilizes deep-learning techniques to introduce an alternative method that facilitates the generation of a substantial droplet dataset. This method is built upon the foundation of a generative adversarial neural network. Additionally, to assess the effectiveness of the proposed method, we establish a deep learning-based droplet detector by leveraging recent advances in computer vision.

### B. Literature review

Over the past decade, deep learning has been developing rapidly with appealing applications across various domains, including finance, medicine, education, and agriculture [7, 8, 9, 10]. In agriculture, these techniques have played a crucial role in addressing complex challenges such as crop detection, fruit segmentation, and produce classification. For instance,



Fig. 1: Application of spray systems in agriculture (image is taken from [www.grainnews.ca](http://www.grainnews.ca))

[11] applied deep-learning algorithms for the detection and segmentation of apples. For crop detection, [12] developed an algorithm capable of tracking crops in sunny conditions.

Beyond the application of machine learning in crop treatment, it also plays an important role in obtaining measurements for optimizing the design of agricultural devices. For example, work in [5, 13] employed deep-learning techniques to estimate the spray cone angles and the characteristics of the droplets. To use these novel methods, data collection is crucial and always a challenge because it requires complicated and expensive set-up and excessive labor costs. Therefore, the accuracy and reliability of the model often depend on the training dataset in terms of both quality and quantity.

To resolve this data-size bottleneck and hence increase the performance of deep learning models, there are several techniques we can use, for example collecting more data, transfer learning, data augmentation, and synthetic data generation [14]. For data augmentation, we can apply transformations to existing data to create new samples, including rotations, flips, zooms, or changes in brightness and contrast. Generally, the performance of the model could be improved by applying the data augmentation techniques. Compared to the data augmentation techniques, synthetic data generation can create new samples based on the original samples. This can be especially beneficial when creating novel patterns or dealing with data from class imbalance.

Generative Adversarial Networks (GANs) have revolutionized content and model generation by introducing a novel framework for training generative models [15]. A GAN model

is usually constructed by two models: a generator and a discriminator. The generator produces images from noise to fool the discriminator, while the discriminator aims to distinguish real images from generated ones. This mechanism is trained until the images generated by the generator resemble real images.

Despite the success of the early GAN models, GAN training can be challenging due to model collapse and instability. Therefore, subsequent GAN models have been developed [16, 17, 18, 19] to address these issues. Although the performance of the models has been improved, the quality of generated images remains limited. Towards the end of 2017, researchers from NVIDIA AI released Progressive GAN (ProGAN) [20], which laid the foundation for later works such as StyleGAN [21] and MSG-GAN [22].

The application of generative models in agriculture has become an alternative to traditional methods, leading to a substantial enhancement in precision agriculture [23, 24, 25]. For example, work in [26] created a new dataset of artificial plants for plant phenotyping by using a generative model. Furthermore, the study in [25] demonstrates that they can achieve an accuracy of 95% using only synthetic data for crop seed phenotyping. By using GAN models, time and resources can be saved compared to traditional data collection methods, which are the key inspirations for this paper.

### C. Contributions

In this study, to address the bottleneck of data limitation in our previous work [5], we propose a method to generate

synthetic droplet images via developing a GAN model. Since droplets are small, generating small objects that have a similar appearance as droplets poses a tremendous challenge for a generative model. Therefore, our approach involves generating high-resolution images from low-resolution ones by leveraging the progressive generative methodology. Additionally, this paper establishes a novel droplet detection method using a cutting-edge deep-learning algorithm trained on the AI-generated synthetic data to measure their size.

The key contributions of our work include:

- To the best of our knowledge, this study is the first attempt to leverage deep learning techniques for generating droplet images and establishing a substantial synthetic droplet dataset.
- The droplet image generator in this work is capable of producing images with a resolution of  $1024 \times 1024$ , which is higher than the original images.
- This work introduces a real-time droplet detection model, trained on synthetic data, capable of identifying small droplets.
- We demonstrate that the integration of synthetic droplet images improves the detector performance by 16.06%.
- This work lays the foundation for integrating modern generative AI methods to address other tasks in agriculture.

The rest of the paper is organized as follows: Section II describes the dataset and data processing. Section III elaborates on the methodologies of deep learning algorithms behind the droplet image generator. In this section, we also discuss the droplet detection algorithm. The model training and metrics for evaluating the performance of the models are explained in Section IV. Section V discusses the results and compares the effects of using a synthetic dataset. Finally, Section VI provides concluding remarks on this work.

## II. EXPERIMENTAL DATASET

Inspired by our prior work [5], we gathered data through an experimental setup with an array of crop spray nozzles capable of producing various spray patterns Fig. 2. In the experiments, we captured images of droplets with a resolution of  $640 \times 640$  sprayed by the nozzles using a high-speed camera operating at 2000 frames per second to construct a droplet database.

The dataset comprises three sets: train (469 images), validation (125 images), and test (124 images). As depicted in Figure 3, the droplet size is substantially smaller than the overall image dimensions. For training the GAN droplet generator, we utilize 400 images from the training dataset as inputs. This GAN generator can subsequently produce up to 5000 synthetic droplet images, as discussed in Section V.

## III. METHODS

Motivated by the need to address the bottleneck of data availability, we developed a model capable of generating droplet images through a generative AI framework. As illustrated in Fig. 3, the droplet sizes are notably small relative to the overall image dimensions. Therefore, our approach is generating high-resolution images from their low-resolution

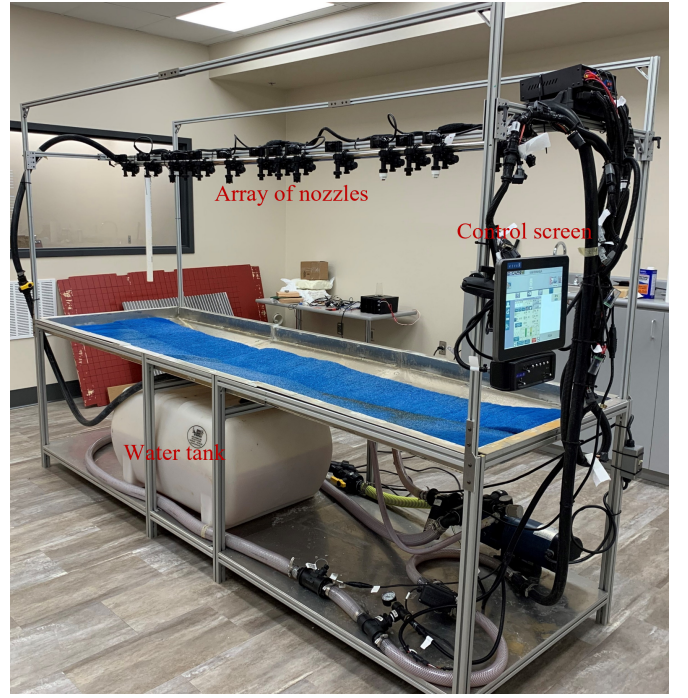


Fig. 2: Experimental setup of a spray system for droplet generation.

counterparts, utilizing the progressive mechanism [20]. This section describes the mechanism and architecture of the model employed in the generation of droplet images.

### A. Droplet generative model

1) *Generative mechanism:* The generative model consists of two networks: a generator  $G$  and a discriminator  $D$ , as shown in Fig. 4. In the training process, the generator tries to generate synthetic data from the noise vector  $z$  that looks similar to real data to fool the discriminator. On the other hand, the discriminator tries to adjust its hyperparameters to distinguish the difference between fake and real data. The parameters of the generator and discriminator are updated constantly during the training. The training process can be formulated as a minimax game between the generator and discriminator as follows:

$$u_i = \min_G \max_D (\mathbb{E}_{x \sim p_{\text{data}}(x)} [\log(D(x))] + \mathbb{E}_{z \sim p_z(z)} [\log(1 - D(G(z)))]).$$

Here,  $p_{\text{data}}(x)$  is the distribution of real data  $x$ , and  $p_z(z)$  is the distribution of the latent noise vector  $z$ .

The model generates droplet images by following the progressive growth mechanism. Specifically, at the initial stages of training, the generator starts generating images with a low resolution, as illustrated in Fig. 5. Then, new layers are incrementally added to the generator as the training progresses, allowing it to capture finer details in the images. Simultaneously, the discriminator also grows, learning to assess the increasing resolution of the generated images. In addition, it is



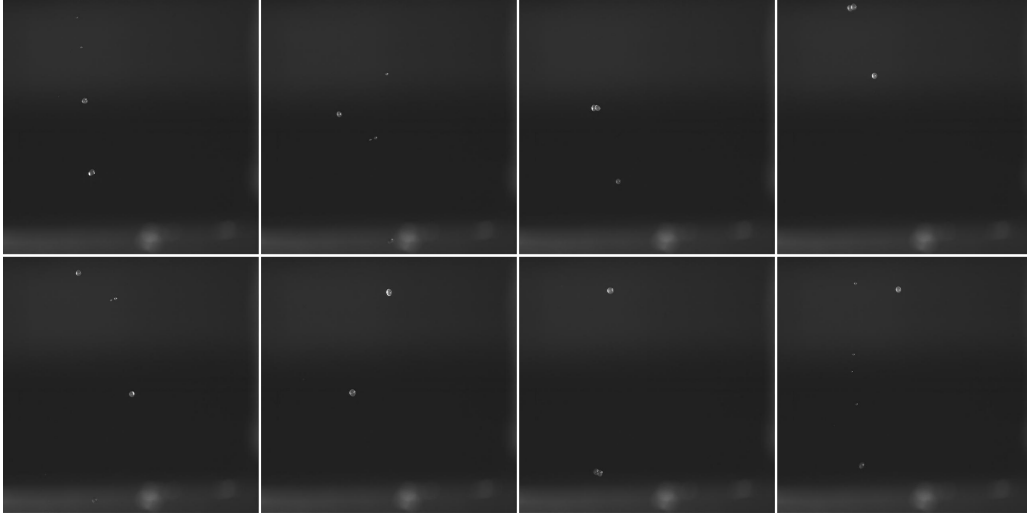


Fig. 3: Droplet images captured from a high-speed camera in the experiments.

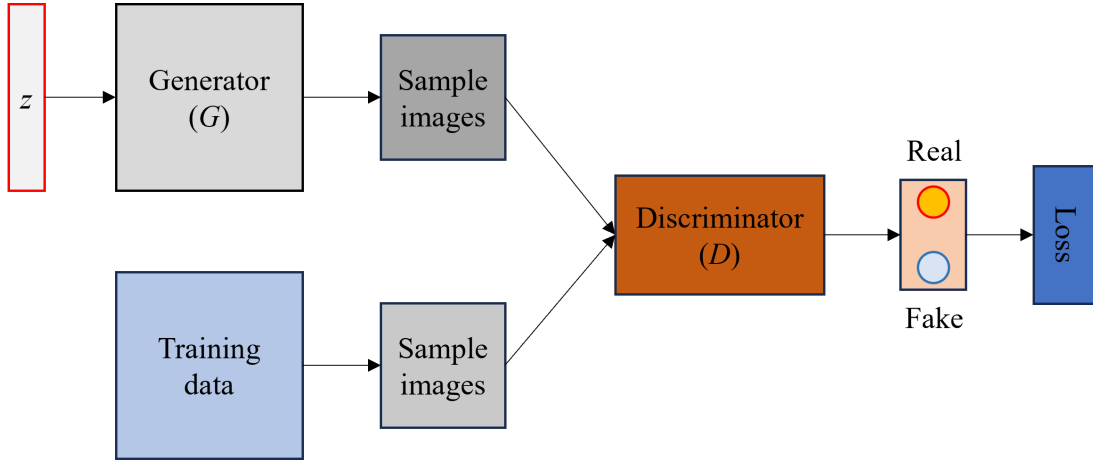


Fig. 4: The architecture of the GAN model. The generator and discriminator are trained together to finalize the best generator.

worth noticing that all existing layers remain trainable during the growth process.

This incremental growth has several advantages. It leads to a more stable training process, mitigating issues such as mode collapse, where the generator produces a limited variety of samples. Additionally, it facilitates the generation of high-quality, high-resolution images, a significant improvement over traditional GANs. In the next sections, we will delve into the structure of the generator and discriminator networks.

2) *Generator*: The generator is a convolutional neural network (CNN) responsible for generating synthetic data. Given a random noise vector  $z$  sampled from a latent space, the generator produces (fake) images  $G(z)$  by using convolution layers that follow the distribution of real training images. Mathematically, this process can be expressed as  $G : z \rightarrow G(z; \theta_g)$ , in which  $\theta_g$  contains the parameters of the generator.

Subsequently, the generator adds more layers to generate

features with higher resolution in the next block as shown in Fig. 5. The added layers in this process are illustrated in Fig. 6a, which includes  $3 \times 3$  convolution layers followed by LeakyReLU (LReLU) and PixelNorm activation functions. Let  $g_i$  be a generic function that acts as the basic generator block, then the output of the block  $g_i$  is

$$A_i \in \mathbb{R}^{2^{i+1} \times 2^{i+1} \times c_i}, 1 \leq i \leq 9, \quad (1)$$

where  $i \in N$ , and  $c_i$  is the number of channels in the generator block  $i$ -th. The progressive training process is repeated until the model generates features with the resolution of  $1024 \times 1024$ . In addition, at the end of the generator, a  $1 \times 1$  convolution layer is applied to generate color images.

For instance, in the first block, the generator creates images with a resolution of  $4 \times 4$  from the latent vector (noise) using convolution layers. Subsequently, the generator upscales the images generated in block 1 to a size of  $8 \times 8$  in block 2. Similar to block 2, this image-generation process is reiterated



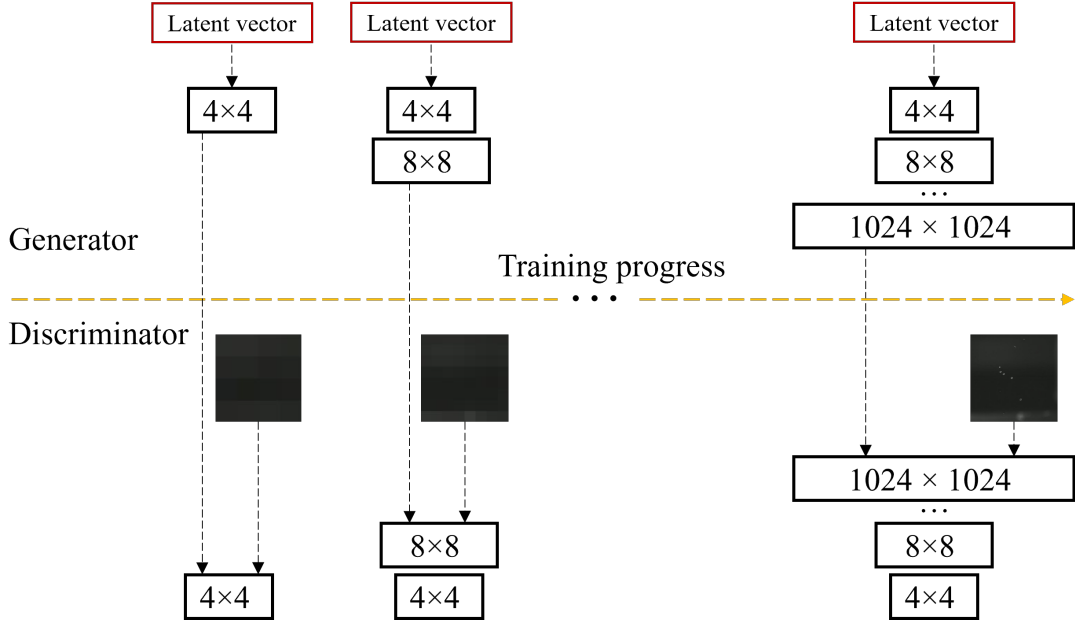


Fig. 5: The architecture of the generative model in the training process.

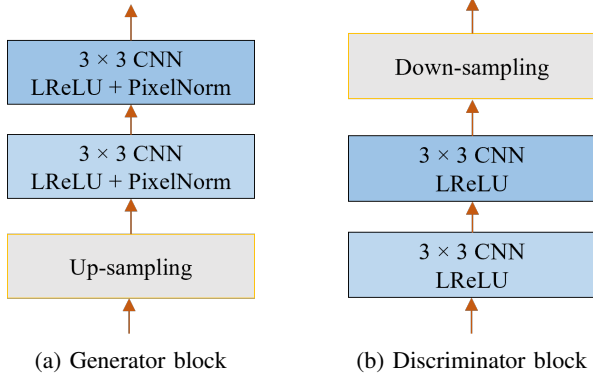


Fig. 6: Generator and discriminator blocks in the progressive generative model.

until reaching the image size of  $1024 \times 1024$ . The progressive mechanism enables the generator to capture intricate features of droplets.

3) *Discriminator*: The discriminator is another convolutional neural network that evaluates whether a given data point is from the actual experiments or generated artificially by the generator. To do that, the discriminator also undergoes a progressive growth process. It starts with an architecture designed for evaluating low-resolution images and then expands its capacity as the resolution of generated images increases during training.

As shown in Fig. 5, given a generated data point  $G(z)$ , the discriminator outputs a probability  $D(G(z))$  indicating the likelihood of  $G(z)$  being a real sample. Mathematically, this can be expressed as  $D : G(z) \rightarrow D(G(z))$ . The initial discriminator network is composed of a  $3 \times 3$  convolution

followed by a  $4 \times 4$  convolution and a fully connected layer. Starting with a low-resolution image of size  $4 \times 4$ , the discriminator processes it using the initial networks and outputs the probability of the input image being real.

Similar to the generator's architecture, additional layers are added to the discriminator's network to handle larger images during the training. Let  $d_i$  represent a basic discriminator block, the architecture of the block  $d_i$  is described in Fig. 6b. This discriminator block consists of two  $3 \times 3$  convolution layers and a down-sampling layer.

During the training process, the discriminator is trained to minimize classification loss, whether the input is generated data or real data. The loss that measures the difference between the predicted probability of input being real and the actual label is formulated as follows:

$$L = \mathbb{E}_{z \sim P_z} [D(G(z))] - \mathbb{E}_{x \sim P_{\text{data}}} [D(x)] + \lambda \mathbb{E}_{\hat{x} \sim P_{\hat{x}}} [(\|\nabla_{\hat{x}} D(\hat{x})\|_2 - 1)^2],$$

where  $P_{\text{data}}$  is the distribution of real samples,  $P_z$  is the distribution of generated samples,  $\hat{x}$  is a random sample along the straight lines between pairs of real and generated samples, and  $\lambda$  is a regularization parameter controlling the strength of the gradient penalty [27].

When designing the discriminator architecture, we employed a reverse engineering approach that aligns with the construction of the generator network. Beginning with an image, the input undergoes a series of neural network layers following the discriminator block until it reaches the real image size [20].

### B. Droplet Detection

In this study, we introduce a droplet detection method leveraging the YOLOv8 object-detection model [28], which

is designed for real-time object detection. Compared to other models, it stands out as an efficient and state-of-the-art model known for its high accuracy and fast processing speed. The model comprises two main components: a backbone and a head.

The **backbone** is an important part of the model, extracting meaningful features from the input image. It consists of 53 convolutional layers arranged in a modified CSPNet architecture [29]. The design of the backbone network enables the model to capture intricate feature maps while remaining lightweight.

Additionally, YOLOv8 integrates a Pyramid Pooling Fast module (SPPF), a feature that reduces computational complexity while preserving feature representation. It incorporates a Path Aggregation Network (PANet) that effectively aggregates features from different scales of the backbone. This allows the model to capture objects of various sizes and resolutions.

The detection **head** is responsible for predicting bounding boxes and class labels for objects in the input image. There are three sub-detection heads in the model, which enable the model to capture objects of different sizes. Furthermore, there is a decoupled head structure in each sub-detection head: one for predicting class labels and the other for predicting bounding boxes. This separation enables the model to focus independently on each task, thereby enhancing the accuracy of both bounding box predictions and object classification.

#### IV. EXPERIMENT AND EVALUATION METRICS

##### A. Evaluation metrics for GAN

To assess the quality of synthetic images produced by the generative model, we employ a qualitative assessment method, and this method contains two essential properties: Fidelity and Diversity. Fidelity is used for assessing the quality of the generated samples, measuring how realistic the images appear. Diversity evaluates the range of the generated samples, assessing how well they cover the entirety of the real distribution's variety [30].

The fidelity and diversity of the synthesized images generated by the generator are evaluated by precision and recall metrics through droplet detection. High precision indicates that the generated images closely resemble real images on average, while high recall suggests that the generator can produce any sample present in the training dataset [31].

##### B. Evaluation metrics for Object detection

In the evaluation process, the trained droplet detector takes in images, detects droplets in the images, and then generates bounding boxes around detected droplets. To evaluate the performance of the detector, we subsequently compared the predictions with the corresponding ground truths. This involves a detailed analysis of the spatial overlap between predicted and ground-truth bounding boxes.

To facilitate the evaluation process, we defined specific parameters as follows:

- True Positive (TP) is the number of correctly predicted droplet bounding boxes compared with the ground truth bounding boxes of droplets.
- False Positive (FP) is the number of incorrectly predicted droplet bounding boxes compared with the ground truth bounding boxes of droplets.
- False Negative (FN) is the number of predicted droplet bounding boxes when the model fails to detect actual droplets present in the image.

Based on the definition above, the evaluation metrics are defined as

$$\text{Precision} = \frac{TP}{TP + FP} \quad (2)$$

$$\text{Recall} = \frac{TP}{TP + FN} \quad (3)$$

where Precision represents the accuracy of positive predictions that is computed as the ratio of TP to the sum of TP and FP. Recall, on the other hand, is the ratio of TP to the sum of TP and FN, indicating the model's ability to capture all positive instances.

Beyond using Precision and Recall metrics, we also use Average Precision (AP) to evaluate the performance of the model. Average Precision is a comprehensive metric that considers precision-recall trade-offs at various confidence thresholds. A higher AP signifies a more robust and reliable droplet detection model. It involves calculating the area under the precision-recall curve and is defined as follows:

$$AP = \int_0^1 \text{Precision}(\text{Recall}) d(\text{Recall}) \quad (4)$$

#### V. RESULTS AND DISCUSSION

##### A. Synthetic Dataset with the generative model

After training with real images, the generator adeptly generated more than 5000 synthetic images with a resolution of  $1024 \times 1024$ . This volume of droplet images would require tremendous resources if generated via experiments. However, not all of these images have high-quality standards, hence, we selected around 1500 images for our subsequent experiments. The representations of these images are illustrated in Fig. 7.

As we observed, these images exhibit a notable resemblance to real ones, illustrating not only in terms of resolution but also in capturing intricate details, including small droplets. The generative model demonstrates its capability to produce realistic droplet images, thereby enriching the database with a diverse array of visual features.

For a more intuitive comparison between generated and real images, we cropped the section containing droplets in the images and presented it in Fig. 8. Specifically, Figure 8a showcases a synthetic image produced by the generative AI model with its corresponding zoomed-in area, while Figure 8b displays a real image from the experiment accompanied by its zoom area. As observed, the zoomed areas reveal subtle distinctions between images, in which the real image shows that the contrast of droplets in the image is higher than in the synthetic image.

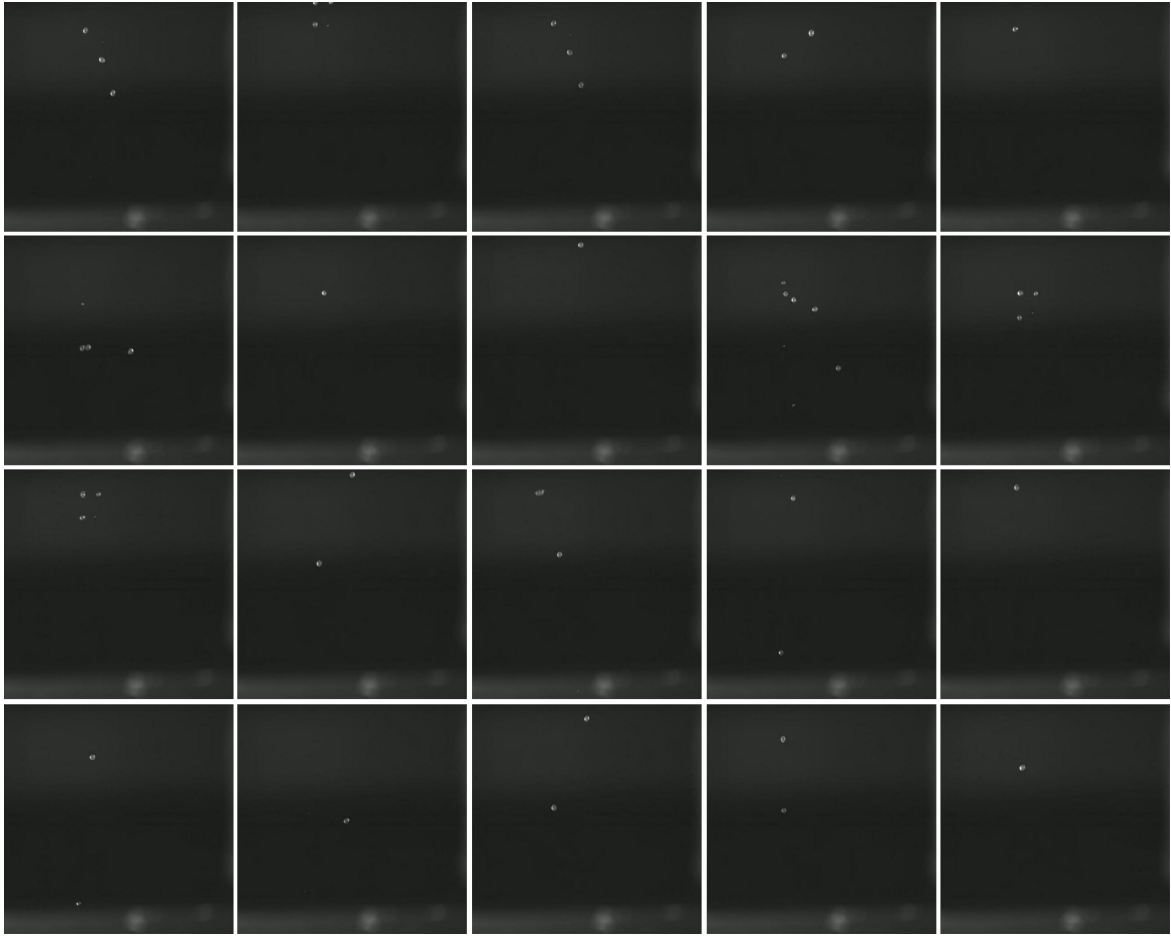


Fig. 7: Droplet images produced by the generative model.

TABLE I: Evaluate the quality of generated images by using Precision (Pre.) and Recall (Rec.) metrics. We used the original dataset (469 training samples) and the synthetic dataset (500 samples) for the comparison.

Data	Validation				Test			
	Pre.	Rec.	mAP50	mAP50-95	Pre.	Rec.	mAP50	mAP50-95
Real (469)	0.920	0.898	0.954	0.635	0.891	0.877	0.950	0.636
Synthetic (500)	0.909	0.888	0.949	0.623	0.87	0.874	0.941	0.612

In addition to the visual results, we conducted a quantitative analysis using metrics discussed in Section IV. Table I details the training of YOLOv8n with 469 real images and 500 synthetic images separately. Moreover, it presents the results of testing these models on validation and test sets. As shown in Table I, Precision and Recall scores are slightly lower when using synthetic images compared to real images, though the difference is not significant. Specifically, the model trained with real data achieves Precision and Recall scores of 0.891 and 0.877, respectively, on the test set, while the model trained with synthetic data achieves a Precision score of 0.87 and a Recall score of 0.874.

#### B. Droplet detection results

After obtaining the synthetic dataset, a series of experiments were conducted to improve droplet detection performance. The results are listed in Table II. Initially, YOLOv8n was trained using the real dataset, comprising 469 images. As shown in Table II, the model achieved an mAP50 of 0.950 and an mAP50-90 of 0.636 on the test set. On the validation set, the corresponding values were 0.954 for mAP50 and 0.635 for mAP50-95.

To leverage the synthetic dataset, we utilized the pre-trained model mentioned above to label the data. It's important to note that the labeled data at this stage may not be perfectly accurate, therefore, we labeled the dataset based on the initial labeled data.



TABLE II: Comparison of droplet detection results between the original dataset and augmented dataset. In this table, “Pre.” and “Rec.” represent Precision and Recall metrics, respectively. Additionally, the detection performance on the real dataset is denoted by (R).

Data	Validation				Test			
	Pre.	Rec.	mAP50	mAP50-95	Pre.	Rec.	mAP50	mAP50-95
469 (R)	0.920	0.898	0.954	0.635	0.891	0.877	0.950	0.636
969	0.955	0.89	0.96	0.685	0.956	0.888	0.970	0.683
1469	0.964	0.916	0.974	0.698	0.948	0.929	0.977	0.704
1783	0.938	0.932	0.966	0.717	0.938	0.927	0.973	0.703
2504	0.969	0.962	0.988	0.737	0.951	0.970	0.988	0.721

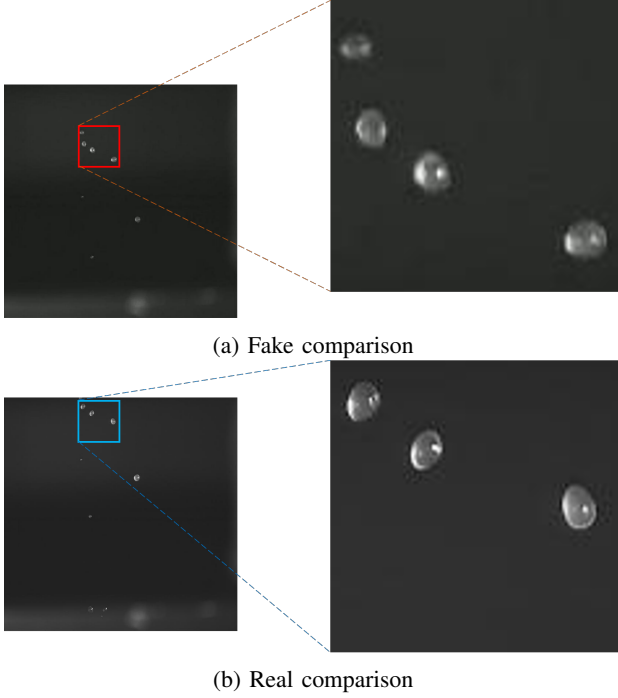


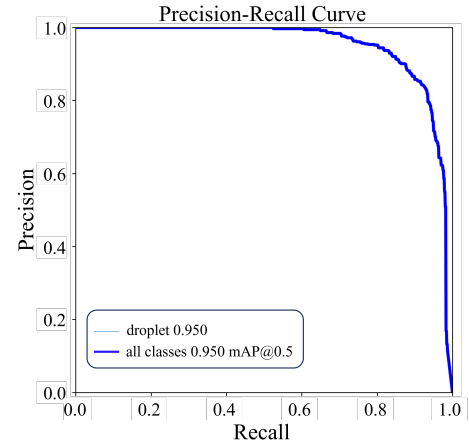
Fig. 8: Comparison of generated images and real images.

To assess the droplet detection effectiveness, we gradually increased the number of training samples by adding synthetic (fake) images, resulting in sizes of 969, 1469, 1783, and 2504 images. Importantly, we kept the number of samples consistent in the validation and test sets.

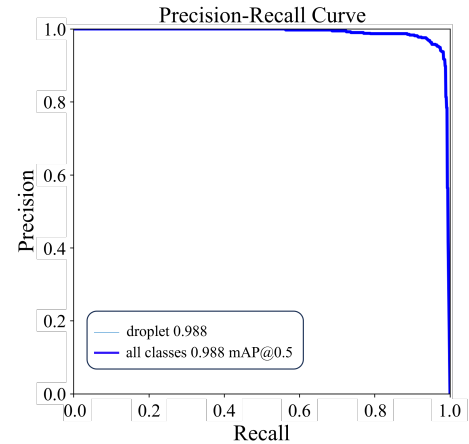
As observed, the detector’s performance improves with the addition of synthetic samples. For example, when combining 469 real images with 500 synthetic images, following the comparison in Table I, the mAP50-95 scores increased by 7.38% on the test set and 7.87% on the validation set. Furthermore, in the case of a 2504-sample training, the mAP50 increased from 0.950 to 0.988, and mAP50-95 increased from 0.636 to 0.721 on the test set compared to the real-sample training. Similarly, a consistent trend is observed in the validation set, where mAP50 increased to 0.988, and mAP50-95 increased to 0.737.

In addition to the results presented in Table II, we compare Precision-Recall (PR) curves between the original training (only real images) and the training with 2504 samples (real

images + synthetic images), as shown in Fig. 9. Notably, the area under the PR curve for the original training is smaller compared to that of the augmented training. Consequently, incorporating generated data into the training set yields improved results.



(a) Precision-Recall curve on original dataset (using only real dataset)



(b) Precision-Recall curve on augmented dataset (using augmented dataset)

Fig. 9: Comparison of droplet detection performance on the test set in terms of the Precision-Recall curve when utilizing an augmented dataset.

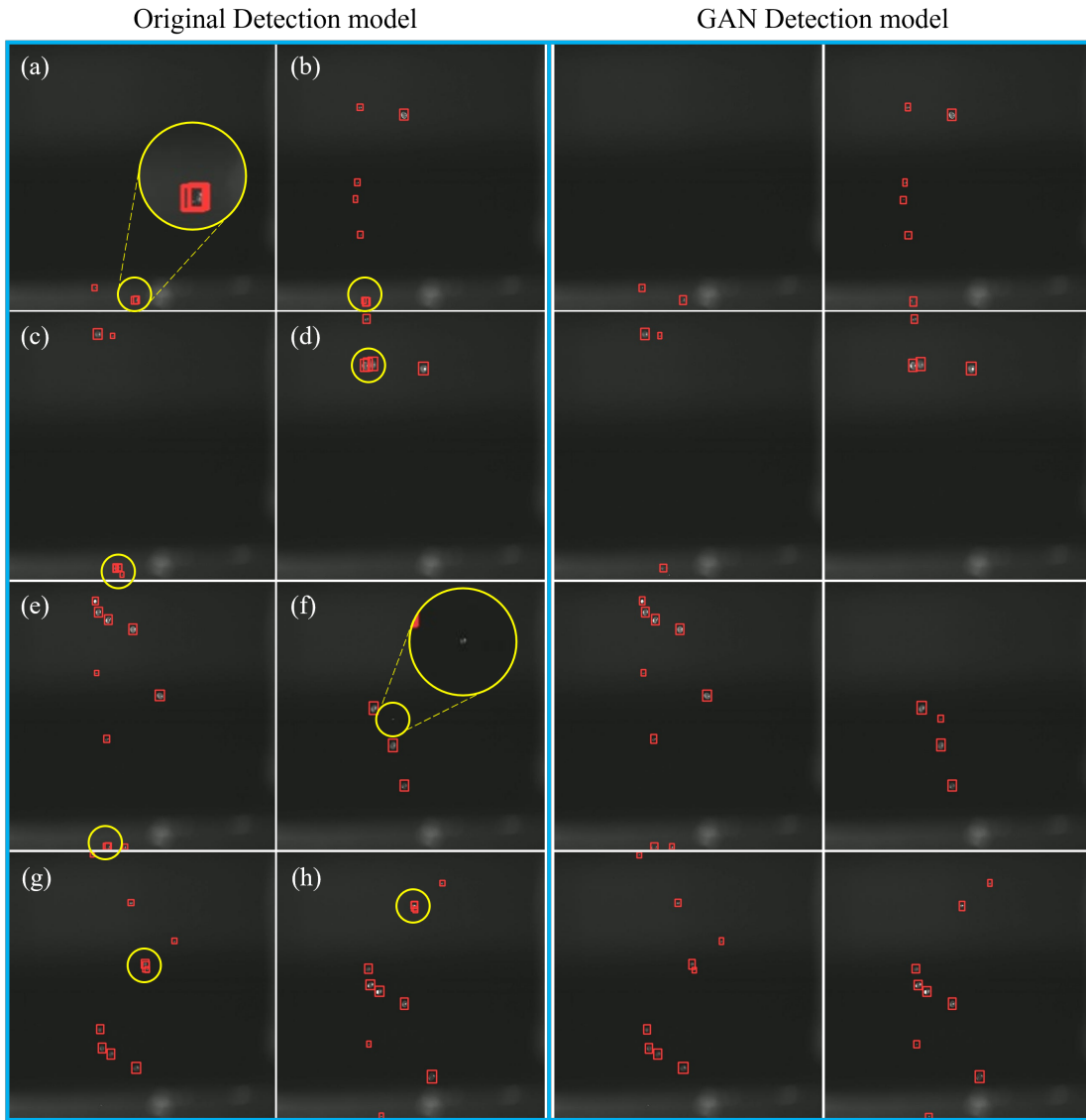


Fig. 10: Prediction comparison based on the original training data (469 samples) and augmented training data (2504 samples). The initial two columns display predictions from the original training, while the last two columns show predictions from the augmented data, corresponding to their counterparts in the first two columns. Typically, the inaccurate predictions are highlighted by yellow circles.

Fig. 10 illustrates the comparative efficacy of droplet detection of the two models, one was trained with only real droplet images and the other was trained with mixed real and synthetic droplets. The first two columns depict the droplet detection results produced by the model trained with only real droplet images (as indicated by the first train case in Table II). The last two columns show the droplet detection results on the same images produced by the model trained with the 2504-sample dataset (mixed real and synthetic images). Moreover, the yellow circles highlight inaccuracies in the detection by the first model.

In particular, when utilizing the augmentation dataset (mixed real and synthetic images) for training, the GAN

model detects droplets more precisely as compared to the original model trained with just real droplet images. As illustrated in the zoomed region of Fig. 10a, the original model predicted one droplet with two bounding boxes, while the GAN detection model predicted exactly one bounding box for a single droplet. This comparison can be observed similarly in Figs. 10b, c, d, e, g, and h. In addition, the GAN detection model can detect all droplets in the images, including small ones that the original model misses, as demonstrated in Fig. 10f.

## VI. CONCLUSION

This work introduces a novel approach to streamline spray system optimization through a data augmentation method. The method uses a generative adversarial neural network to create a synthetic dataset. The generative model consists of a generator and a discriminator: the generator produces images from noise to fool the discriminator; the discriminator tries to distinguish images generated by the generator and the real images.

To train the generative AI model, we collect data from experiments using a high-speed camera to capture droplet images. Instead of initially training the generator to produce high-resolution images, the training process begins with the generator creating images at a small resolution of  $4 \times 4$  and gradually increasing it up to  $1024 \times 1024$ . This progressive training facilitates the model in learning features at different scales, enhancing its stability and ability to generate high-quality images.

After obtaining the synthesized dataset, we labeled it using a pre-trained model. To accomplish this, we trained YOLOv8-n with the original images and then used the pre-trained model to label the synthetic dataset. Notably, the labeled synthetic data from this process is not of high quality. Therefore, we re-labeled the dataset based on the automatically labeled data.

After getting the dataset, we conducted a series of experiments for droplet detection with models trained with different datasets, including one with only real images and several with a mixture of real and synthetic images. First, we trained the droplet detection model with the original dataset composed of only real images. After that, we gradually added an amount of synthetic data to the initial training dataset. The results show that the detection performance is improved as the number of synthetic images increases. Specifically, the model achieved mAP50 and mAP50-90 scores of 0.950 and 0.636 on the original dataset while these metrics in the case of mixed-data training are 0.988 and 0.721, respectively.

Although the model can generate more datasets, they are limited to a few varieties. Therefore, in the future, we aim to find a way to generate a dataset with greater diversity. We plan to build a larger database for droplet images based on the generative model and use our model to automate the labeling process. Additionally, we will apply the droplet detector to estimate droplet characteristics during the nozzle optimization design process.

## REFERENCES

- [1] B. Balewski, B. Heine, and C. Tropea, "Experimental investigation of the correlation between nozzle flow and spray using laser doppler velocimeter, phase doppler system, high-speed photography, and x-ray radiography," *Atomization and Sprays*, vol. 20, no. 1, 2010.
- [2] T. Kawaguchi, Y. Akasaka, and M. Maeda, "Size measurements of droplets and bubbles by advanced interferometric laser imaging technique," *Measurement Science and Technology*, vol. 13, no. 3, p. 308, 2002.
- [3] B. Schmandt and H. Herwig, "Diffuser and nozzle design optimization by entropy generation minimization," *Entropy*, vol. 13, no. 7, pp. 1380–1402, 2011.
- [4] C. Goddeeris, F. Cuppo, H. Reynaers, W. Bouwman, and G. Van den Mooter, "Light scattering measurements on microemulsions: estimation of droplet sizes," *International journal of pharmaceutics*, vol. 312, no. 1-2, pp. 187–195, 2006.
- [5] P. Acharya, T. Burgers, and K.-D. Nguyen, "Ai-enabled droplet detection and tracking for agricultural spraying systems," *Computers and Electronics in Agriculture*, vol. 202, p. 107325, 2022.
- [6] L. Wang, W. Song, Y. Lan, H. Wang, X. Yue, X. Yin, E. Luo, B. Zhang, Y. Lu, and Y. Tang, "A smart droplet detection approach with vision sensing technique for agricultural aviation application," *IEEE Sensors Journal*, vol. 21, no. 16, pp. 17 508–17 516, 2021.
- [7] A. M. Ozbayoglu, M. U. Gudelek, and O. B. Sezer, "Deep learning for financial applications: A survey," *Applied Soft Computing*, vol. 93, p. 106384, 2020.
- [8] T.-H. Pham, X. Li, and K.-D. Nguyen, "Seunet-trans: A simple yet effective unet-transformer model for medical image segmentation," *arXiv preprint arXiv:2310.09998*, 2023.
- [9] P. Bhardwaj, P. Gupta, H. Panwar, M. K. Siddiqui, R. Morales-Menendez, and A. Bhaik, "Application of deep learning on student engagement in e-learning environments," *Computers & Electrical Engineering*, vol. 93, p. 107277, 2021.
- [10] T.-H. Pham, P. Acharya, S. Bachina, K. Osterloh, and K.-D. Nguyen, "Deep-learning framework for optimal selection of soil sampling sites," *Computers and Electronics in Agriculture*, vol. 217, p. 108650, 2024.
- [11] Y. Tian, G. Yang, Z. Wang, H. Wang, E. Li, and Z. Liang, "Apple detection during different growth stages in orchards using the improved yolo-v3 model," *Computers and electronics in agriculture*, vol. 157, pp. 417–426, 2019.
- [12] E. Hamuda, B. Mc Ginley, M. Glavin, and E. Jones, "Improved image processing-based crop detection using kalman filtering and the hungarian algorithm," *Computers and electronics in agriculture*, vol. 148, pp. 37–44, 2018.
- [13] P. Acharya, T. Burgers, and K.-D. Nguyen, "A deep-learning framework for spray pattern segmentation and estimation in agricultural spraying systems," *Scientific Reports*, vol. 13, no. 1, pp. 1–14, 2023.
- [14] C. Shorten and T. M. Khoshgoftaar, "A survey on image data augmentation for deep learning," *Journal of big data*, vol. 6, no. 1, pp. 1–48, 2019.
- [15] I. Goodfellow, J. Pouget-Abadie, M. Mirza, B. Xu, D. Warde-Farley, S. Ozair, A. Courville, and Y. Bengio, "Generative adversarial nets," *Advances in neural information processing systems*, vol. 27, 2014.
- [16] A. Radford, L. Metz, and S. Chintala, "Unsupervised representation learning with deep convolutional generative



- adversarial networks,” *arXiv preprint arXiv:1511.06434*, 2015.
- [17] T. Salimans, I. Goodfellow, W. Zaremba, V. Cheung, A. Radford, and X. Chen, “Improved techniques for training gans,” *Advances in neural information processing systems*, vol. 29, 2016.
  - [18] M.-Y. Liu and O. Tuzel, “Coupled generative adversarial networks,” *Advances in neural information processing systems*, vol. 29, 2016.
  - [19] J.-Y. Zhu, T. Park, P. Isola, and A. A. Efros, “Unpaired image-to-image translation using cycle-consistent adversarial networks,” in *Proceedings of the IEEE international conference on computer vision*, 2017, pp. 2223–2232.
  - [20] T. Karras, T. Aila, S. Laine, and J. Lehtinen, “Progressive growing of gans for improved quality, stability, and variation,” *arXiv preprint arXiv:1710.10196*, 2017.
  - [21] T. Karras, S. Laine, and T. Aila, “A style-based generator architecture for generative adversarial networks,” in *Proceedings of the IEEE/CVF conference on computer vision and pattern recognition*, 2019, pp. 4401–4410.
  - [22] A. Karnewar and O. Wang, “Msg-gan: Multi-scale gradients for generative adversarial networks,” in *Proceedings of the IEEE/CVF conference on computer vision and pattern recognition*, 2020, pp. 7799–7808.
  - [23] D. Ward, P. Moghadam, and N. Hudson, “Deep leaf segmentation using synthetic data,” *arXiv preprint arXiv:1807.10931*, 2018.
  - [24] B. Espejo-Garcia, N. Mylonas, L. Athanasakos, E. Vali, and S. Fountas, “Combining generative adversarial networks and agricultural transfer learning for weeds identification,” *Biosystems Engineering*, vol. 204, pp. 79–89, 2021.
  - [25] Y. Toda, F. Okura, J. Ito, S. Okada, T. Kinoshita, H. Tsuji, and D. Saisho, “Training instance segmentation neural network with synthetic datasets for crop seed phenotyping,” *Communications biology*, vol. 3, no. 1, p. 173, 2020.
  - [26] M. Valerio Giuffrida, H. Scharr, and S. A. Tsaftaris, “Arigan: Synthetic arabidopsis plants using generative adversarial network,” in *Proceedings of the IEEE international conference on computer vision workshops*, 2017, pp. 2064–2071.
  - [27] I. Gulrajani, F. Ahmed, M. Arjovsky, V. Dumoulin, and A. C. Courville, “Improved training of wasserstein gans,” *Advances in neural information processing systems*, vol. 30, 2017.
  - [28] G. Jocher, A. Chaurasia, and J. Qiu, “YOLO by Ultralytics,” Jan. 2023. [Online]. Available: <https://github.com/ultralytics/ultralytics>
  - [29] J. Redmon and A. Farhadi, “Yolov3: An incremental improvement,” *arXiv preprint arXiv:1804.02767*, 2018.
  - [30] Q. Xu, G. Huang, Y. Yuan, C. Guo, Y. Sun, F. Wu, and K. Weinberger, “An empirical study on evaluation metrics of generative adversarial networks,” *arXiv preprint arXiv:1806.07755*, 2018.
  - [31] M. Lucic, K. Kurach, M. Michalski, S. Gelly, and O. Bousquet, “Are gans created equal? a large-scale study,” *Advances in neural information processing systems*, vol. 31, 2018.